Journal of Hazardous Materials 195 (2011) 261–275

Contents lists available at SciVerse ScienceDirect

Journal of Hazardous Materials

journal homepage: www.elsevier.com/locate/jhazmat

Synthesis of a novel silica-supported dithiocarbamate adsorbent and its properties for the removal of heavy metal ions

Lan Bai[a], Huiping Hu[a,*], Weng Fu[a], Jia Wan[a], Xiliang Cheng[b], Lei Zhuge[b], Lei Xiong[b], Qiyuan Chen[a]

[a] School of Chemistry and Chemical Engineering, Central South University, Changsha 410083, China
[b] School of Metallurgical Science and Engineering, Central South University, Changsha 410083, China

ARTICLE INFO

Article history:
Received 8 December 2010
Received in revised form 12 August 2011
Accepted 12 August 2011
Available online 22 August 2011

Keywords:
Heavy metal
Silica-supported dithiocarbamate
Adsorption
Thermodynamics

ABSTRACT

Silica-supported dithiocarbamate adsorbent (Si-DTC) was synthesized by anchoring the chelating agent of macromolecular dithiocarbamate (MDTC) to the chloro-functionalized silica matrix (SiCl), as a new adsorbent for adsorption of Pb(II), Cd(II), Cu(II) and Hg(II) from aqueous solution. The surface characterization was performed by FT-IR, XPS, SEM and elemental analysis indicating that the modification of the silica surface was successfully performed. The effects of media pH, adsorption time, initial metal ion concentration and adsorption temperature on adsorption capacity of the adsorbent had been investigated. Experimental data were exploited for kinetic and thermodynamic evaluations related to the adsorption processes. The characteristics of the adsorption process were evaluated by using the Langmuir, Freundlich and Dubinin–Radushkevich (D–R) adsorption isotherms and adsorption capacities were found to be 0.34 mmol g^{-1}, 0.36 mmol g^{-1}, 0.32 mmol g^{-1} and 0.40 mmol g^{-1} for Pb(II), Cd(II), Cu(II) and Hg(II), respectively. The adsorption mechanism of Hg(II) onto Si-DTC is quite different from that of Pb(II), Cd(II) or Cu(II) onto Si-DTC, which is demonstrated by the XPS and FT-IR results.

1. Introduction

Heavy metals are persistent pollutants because of the toxic, non-biodegradable, accumulative and mobile characters. Due to the rapid increase of the industrial and mining activities which are responsible for the growing metal content in surface and ground water, heavy metal pollution of water bodies has become a serious problem in the world [1]. Many physicochemical methods have been proposed for toxic heavy metal removal from aqueous solution, including chemical precipitation, reverse osmosis, electrochemical reduction, ion exchange and adsorption [2–5].

Among these methods, adsorption is generally preferred for the removal of heavy metal ions due to its high efficiency, easy handling, availability of different adsorbents and cost effectiveness. As one of the adsorbent materials, chelating resin is reusable, easy to be separated, and often has high adsorption capacities [6]. Thus, much attention has been drawn to the synthesis of chelating resins and the investigation of their adsorption behaviors of metal ions from various matrices [7–9]. The dithiocarbamates, due to its strong binding ability to heavy metals while not complexing alkali and alkaline earth metals [10], have been widely used in the environment treatment and have got a good effect in the removal and preconcentration of heavy metals [11–13].

Silica-based organic/inorganic materials have been well studied with attractive characteristics of high chemical reactivity and good mechanical stability [14]. Due to the silanol groups (Si-OH) distributed on the silica gel surface, the silica-supported resins have favorable hydrophilicity, thus leading to higher adsorption efficiency and faster ion diffusion rate than the other resins supported by polystyrene, polyamide, polyvinyl chloride, etc. [15,16].

Most of the reported works about the synthesis of silica-supported dithiocarbamate resins have concerned to add carbon disulfide to modify the surface of silica gel phases containing amine moieties. However, the reaction between carbon disulfide and the amines modified on the silica gel surface is generally conducted under harsh conditions, using of strong alkaline conditions, which results in the degradation of silica matrix [17]. In addition, the great majority of the active amines are polyamine compounds with small molecular weight, such as ethanediamine, diethylenetriamine and triethylenetetramine, which may lead to the less amount of the dithiocarbamate groups on the silica [14,18,19].

In this paper, a new silica-supported dithiocarbamate adsorbent (Si-DTC) was synthesized following a novel synthesis route: a kind of macromolecular dithiocarbamate (MDTC) was synthesized through the reaction of polyethyleneimine with carbon disulfide under strong alkaline conditions and then immobilized onto the chloro-functionalized silica matrix (SiCl) which had

* Corresponding author. Tel.: +86 731 88877364; fax: +86 731 88879616.
E-mail address: phuhuiping@126.com (H. Hu).

0304-3894/$ – see front matter © 2011 Elsevier B.V. All rights reserved.
doi:10.1016/j.jhazmat.2011.08.038

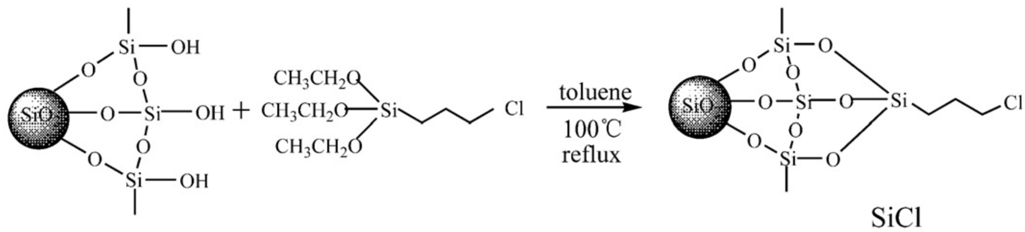

Scheme 1. Synthesis of chloro-functionalized silica gel (SiCl).

been modified by γ-chloropropyltriethoxysilane. By adopting this method, the improvement of the nucleophilic reaction rate of polyethyleneimine with carbon disulfide under the strong alkaline condition could be achieved and the degradation of silica matrix could be avoided. The synthesized adsorbents were used to remove Pb(II), Cd(II), Cu(II) and Hg(II), which are known to be common heavy metals from aqueous solution, and the corresponding removal performance has been studied. In addition, the adsorption characteristics and thermodynamic properties of the adsorbent were examined.

2. Experimental

2.1. Materials

The silica gel used was of chromatographic grade (100–120 mesh size), obtained from Qingdao Haiyang Chemical Co., Ltd., Qingdao, Shandong Province, China. γ-Chloropropyltriethoxysilane (CPTS) was purchased from Xiya Chemical Factory, Chengdu, Sichuan Province, China. Polyethyleneimine (PEI, molecular weight = 1000, 50 wt% aqueous solution) was purchased from Saibo Chemical Factory, Wuhan, Hubei Province, China. Metal salts of $CuSO_4{\cdot}5H_2O$, $Pb(NO_2)_2$, $3CdSO_4\,7H_2O$ and $HgSO_4$ which used to prepare metal ion stock solutions were obtained from Sinopharm Group Chemical Reagent Co. Ltd., Shanghai, China. The stock solutions of Pb(II), Cd(II), Cu(II) and Hg (II) (25 mmol L^{-1} for each ion) were prepared by dissolving appropriate amounts of metal salts in deionized water. The working solutions ranged from 0.25 mmol L^{-1} to 3.0 mmol L^{-1} of the metal ions were prepared by diluting the stock solutions to appropriate volumes. All the other reagents used were of analytical reagent grade except the silica gel.

2.2. Apparatus

Infrared spectra were obtained on a Nicolet 6700 Fourier Transform Infrared Spectrophotometer (Thermo Scientific Co., USA), using KBr pellets in the 4000–400 cm^{-1} region with a resolution of 4 cm^{-1}, by accumulating 16 scans. X-ray photoelectron spectroscopy measurements were carried out on a K-Alpha 1063 XPS spectrometer (Thermo Scientific Co., USA). A monochromatic Al Kα X-ray source (1253.6 eV of photons) was used, with a spot area of

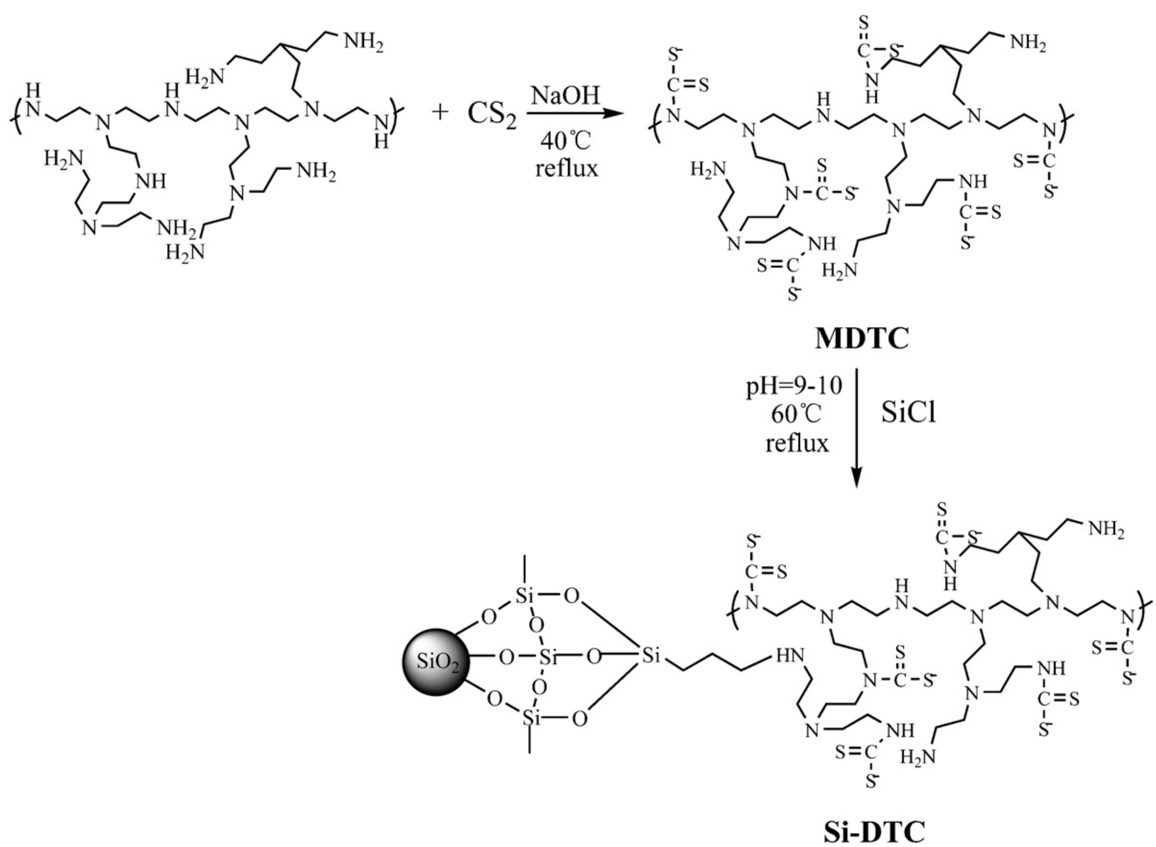

Scheme 2. Synthesis of silica-supported dithiocarbamate adsorbent (Si-DTC).

400 μm. The base pressure in the working chamber was less than 10^{-12} Pa. All binding energies were referenced to the neutral C_{1s} peak at 284.6 eV to compensate for the surface-charging effects. The data from XPS were analyzed by the XPSpeak 4.1 software. A Shirley baseline was used for the subtraction of the background, and Gaussian/Lorentzian (80/20) peaks were used for spectral decomposition. Elemental analysis of C, H, N and S for Si-DTC were subjected to be analyzed by the SC600 Carbon/Sulfur Determinator (LECO Co., USA) and TCH600 Nitrogen/Oxygen/Hydrogen Determinator (LECO Co., USA). The morphology of the adsorbents was examined on JSM-6360LV scanning electron microscope (JEOL Co., Japan). The concentrations of metal ions were determined by an IRIS Intrepid II XSP inductively coupled plasma spectrometer (Thermo Scientific Co., USA) for Hg(II) and a flame atomic absorption spectrophotometer TAS-990F (Beijing Purkinje General Instrument Co., Ltd., China) for Pb(II), Cd(II) and Cu(II). The pH values of metal ion solutions were measured with a pHS-3C digital pH meter (Shanghai Precision & Scientific Co. Ltd., China).

2.3. Synthesis of silica-supported dithiocarbamate adsorbent

2.3.1. Synthesis of SiCl

The chloro-functionalized silica gel (SiCl) was prepared as described in literature [20]. The silica gel (30 g) was first activated with 1 mol L^{-1} nitric acid (200 mL) by refluxing at 50 °C stirring for 6 h. Afterwards the silica gel was washed with deionized water and methanol then the activated silica was air dried overnight. Activated silica gel (5 g) was dispersed into dry toluene (80 mL) in a three-necked round-bottomed flask of total volume 250 mL. CPTS (12.5 mL) and dry toluene (40 mL) were well mixed in a separating funnel and then slowly poured into the flask with continuous stirring. The suspension was mechanically stirred under reflux of the solvent at 100 °C in N_2 atmosphere for 48 h. The final product chloro-functionalized silica (SiCl), was filtered off, washed with toluene and methanol, extracted 6 hours by Soxhlet extraction with methanol at 90 °C, and dried under vacuum at 50 °C for 12 h successively. The reaction scheme is represented in Scheme 1.

2.3.2. Synthesis of MDTC

Under certain conditions, dithiocarbamate was synthesized by the reaction of PEI with carbon disulfide and sodium hydroxide [21]. NaOH (21 g) dissolved in deionized water (50 mL) was added dropwise into a mixture of PEI (15 mL) and methanol (50 mL) in a three-necked round-bottomed flask of total volume 250 mL under ice-bath with continuous mechanical stirring. Excess solution of carbon disulfide (30 mL) and ethanol (50 mL) were well mixed in a beaker and added dropwise through a funnel into the flask with continuous stirring. After all the reagents had been added into the flask, the mixture was heated to 40 °C stirring for 22 h. As the reaction going on, the color of reaction solution changed from faint yellow to orangered. The synthesized product, macromolecular dithiocarbamate (MDTC), was white sodium salt and precipitated at the bottom of the flask. Then the MDTC was filtered and washed with methanol and air dried overnight.

2.3.3. Synthesis of Si-DTC

MDTC (10 g) was dissolved in deionized water (100 mL) in a three-necked round-bottomed flask and the pH of the MDTC solution was checked and adjusted to between 9 and 10 pH units by manually dropwise adding 0.1 mol L^{-1} sulfuric acid in methanol. Then SiCl (3 g) was dispersed into the flask and the suspension refluxed under 60 °C for 10 h. The final product, silica-supported dithiocarbamate adsorbent (Si-DTC), was filtered off, washed with deionized water and methanol, and dried under vacuum at 50 °C for 12 h. The reaction scheme is represented in Scheme 2.

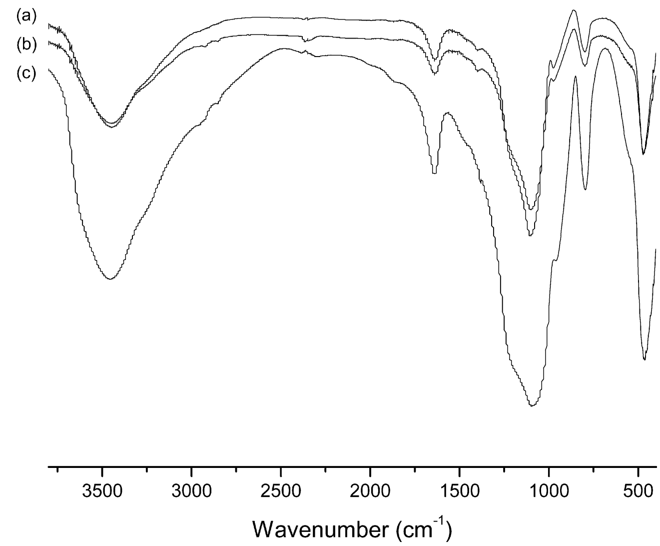

Fig. 1. FT-IR spectra of activated silica gel (a), SiCl (b) and Si-DTC (c).

2.4. Adsorption experiments

Static adsorption experiment was employed to determine the adsorption capability of Si-DTC. The experiments were carried out by shaking 0.05 g of adsorbent with 20 mL of working solution with a certain metal ion concentration. The pH of the working solutions were adjusted adding diluted solution of nitric acid (for Hg(II)) or sulfuric acid (for Pb(II), Cd(II), Cu(II)) and sodium hydroxide, the acetic-acid–sodium-acetate buffer solutions were used when required. The samples were shaken for predetermined time period at a certain temperature and the solid was separated by filtration. Temperature experiments were carried out in a constant-temperature water bath oscillator at the temperature ranged from 303 K to 353 K. Initial and equilibrium metal ion concentrations in the aqueous solutions were determined by using flame atomic absorption spectrometer (AAS) for Pb(II), Cd(II), Cu(II) and inductively coupled plasma spectrometer (ICP) for Hg(II). The amount of metal ions adsorbed by Si-DTC was calculated according to the following Eq. (1):

$$Q = \frac{(C_0 - C)}{W}, \quad (1)$$

where Q is the amount of metal ions adsorbed onto unit amount of the Si-DTC (mmol g^{-1}), C_0 and C are the initial and equilibrium concentrations of the metal ions in aqueous phase (mmol L^{-1}), respectively. V is the volume of the aqueous phase (L), and W is the dry weight of the adsorbent (g).

The adsorption kinetics on the uptake of metal ions by resins was studied by placing 0.20 g resins with 100 mL working solution in a flask. 1 mL solution was taken at different time intervals and the concentration of metal ion was determined by AAS or ICP.

3. Results and discussion

3.1. Characterization of the adsorbent

3.1.1. FT-IR

Fig. 1 shows the FT-IR spectra of activated silica gel (a), SiCl (b) and Si-DTC (c). A large broad band between 3600 cm^{-1} and 3200 cm^{-1} was attributed to the presence of the O–H stretching frequencies of silanol groups and also to the remaining adsorbed water. The sharp features around 1100 cm^{-1} and 462 cm^{-1} indicate Si–O–Si stretching vibrations and bending vibrations, respectively [22]. A characteristic feature of the SiCl when compared with the

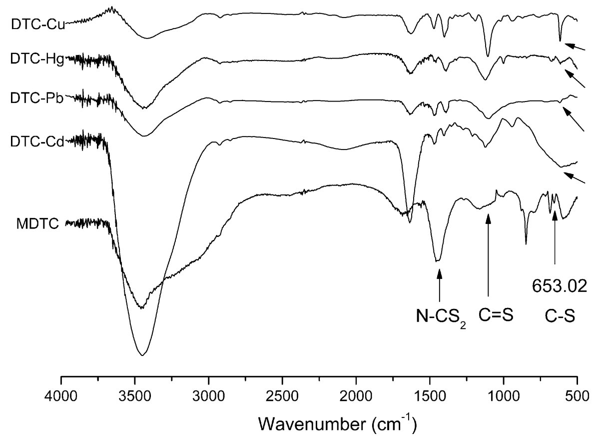

Fig. 2. FT-IR spectra of MDTC, DTC-Pb, DTC-Cd, DTC-Cu and DTC-Hg.

activated silica gel was aliphatic C–H stretching frequencies at 2920 cm^{-1} and 2846 cm^{-1}, indicating that organic silane had been grafted onto the surface of silica gel. There were no prominent features of the dithiocarbamate group in the FT-IR spectra of Si-DTC because they were obscured by the strong absorption peaks of silica gel matrix around 1100 cm^{-1} and 470 cm^{-1}. Thus, the structure of MDTC and the metal chelate complexes of MDTC (DTC-Pb, DTC-Cd, DTC-Cu and DTC-Hg) were confirmed through FT-IR.

Fig. 2 shows the FT-IR spectra of MDTC, DTC-Pb, DTC-Cd, DTC-Cu and DTC-Hg. The characteristic adsorption peaks appearing at 1165 cm^{-1}, 653 cm^{-1} and 1453 cm^{-1} were attributed to C=S vibration, C–S vibration and N–CS_2 vibration, respectively [12,21,23]. The vibration frequencies of C=S and C–S for DTC-Pb, DTC-Cd, DTC-Cu and DTC-Hg shifted to lower frequencies while the N–CS_2 vibration shifted to higher frequencies when compared with MDTC. All of these indicate that a stronger metal-ligand bond had formed between metal ions and chelating groups in MDTC [24]. The characteristic absorption frequencies were summarized in Table 1.

3.1.2. XPS

X-ray photoelectron spectroscopy (XPS) was performed to determine the chemical composition of the adsorbent surface. A portion of the wide-scan XPS spectra for the activated silica gel (a), SiCl (b) and Si-DTC (c) were shown in Fig. 3. The contents (expressed as atomic percent) of Si, O, C, Cl, S and N on the surface of activated silica gel, SiCl and Si-DTC were listed in Table 2.

From Table 2, the contents of Si and O in SiCl and Si-DTC decreased because the silica matrix was covered with organic functional groups. The Cl element was not detected on the surface of Si-DTC, indicating that the Cl atom of SiCl was almost completely

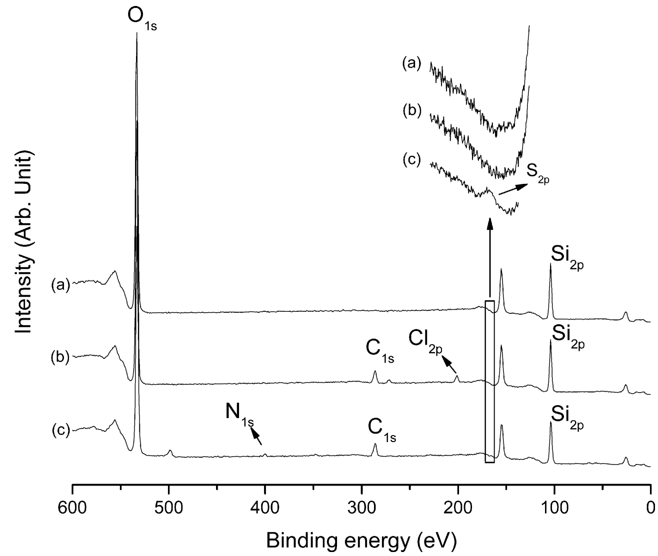

Fig. 3. The XPS spectra of activated silica gel (a), SiCl (b) and Si-DTC (c).

substituted by MDTC during the synthesis of Si-DTC. Because of the high reactivities between SiCl and the amino groups of PEI which had not been subjected to dithiocarbamation, the MDTC should be attached to the surface of SiCl by C–N bond to form Si-DTC (as shown in Scheme 2). However, if the Cl atom of SiCl had been only substituted by N atom from MDTC, the content of N in Si-DTC should not have been less than the content of Cl in SiCl. Actually, from Table 2, the content of N (1.24 at.%) in Si-DTC is lower than the content of Cl (1.54 at.%) in SiCl. Therefore, we can infer that the covalent attachment between MDTC and SiCl was carried out by C–N bond and C–S bond, because the dithiocarbamate groups in MDTC contain a negative ion form and can interact with C–Cl bond of SiCl to form Si-DTC-1 through a new kind of C–S bond (as shown in Scheme 3).

3.1.3. SEM

The SEM images of the activated silica gel (A and B), SiCl (C and D), Si-DTC (E and F) were shown in Fig. 4.

It could be seen that the morphology of the three samples were similar, demonstrating that the silica gel have good mechanical stability and they have not been destroyed during the whole reaction. There appeared more multihole structures on the surface of Si-DTC (F) comparing with that of activated silica gel (B) and Si-Cl (D), mainly because of the microcorrosion of the silica matrix surface by the solution with pH values of 9–10 during the synthesis of Si-DTC.

Table 1
The absorption frequencies of MDTC, DTC-Pb, DTC-Cd, DTC-Cu and DTC-Hg.

Group	Strength	Absorption frequencies				
		MDTC	DTC-Pb	DTC-Cd	DTC-Cu	DTC-Hg
C=S	Strong	1165.48	1098.22	1117.44	1107.01	1123.84
C–S	Weak	653.02	617.19	614.21	617.79	611.39
N–CS_2	Very strong	1453.74	1462.40	1466.55	1472.95	1456.94

Table 2
The surface compositional data from XPS.

Samples	XPS analysis (at.%)					
	Si_{2p}	O_{1s}	C_{1s}	Cl_{2p}	N_{1s}	S_{2p}
Activated silica gel	33.29	66.71	–	–	–	–
SiCl	29.89	59.83	8.75	1.54	–	–
Si-DTC	29.45	59.94	9.07	–	1.24	0.3

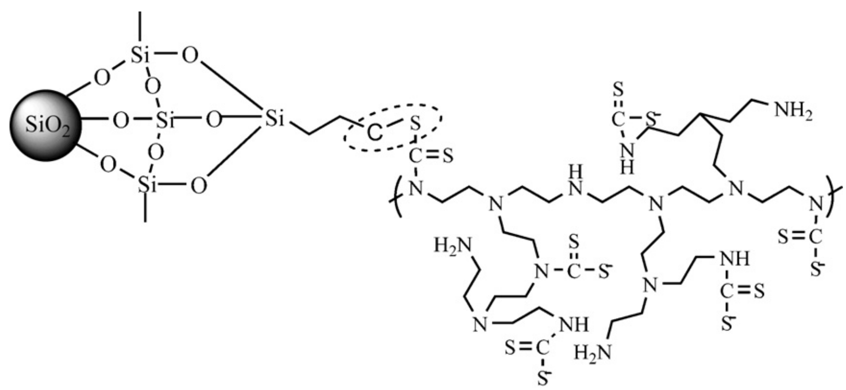

Si-DTC-1

Scheme 3. The structure of Si-DTC-1.

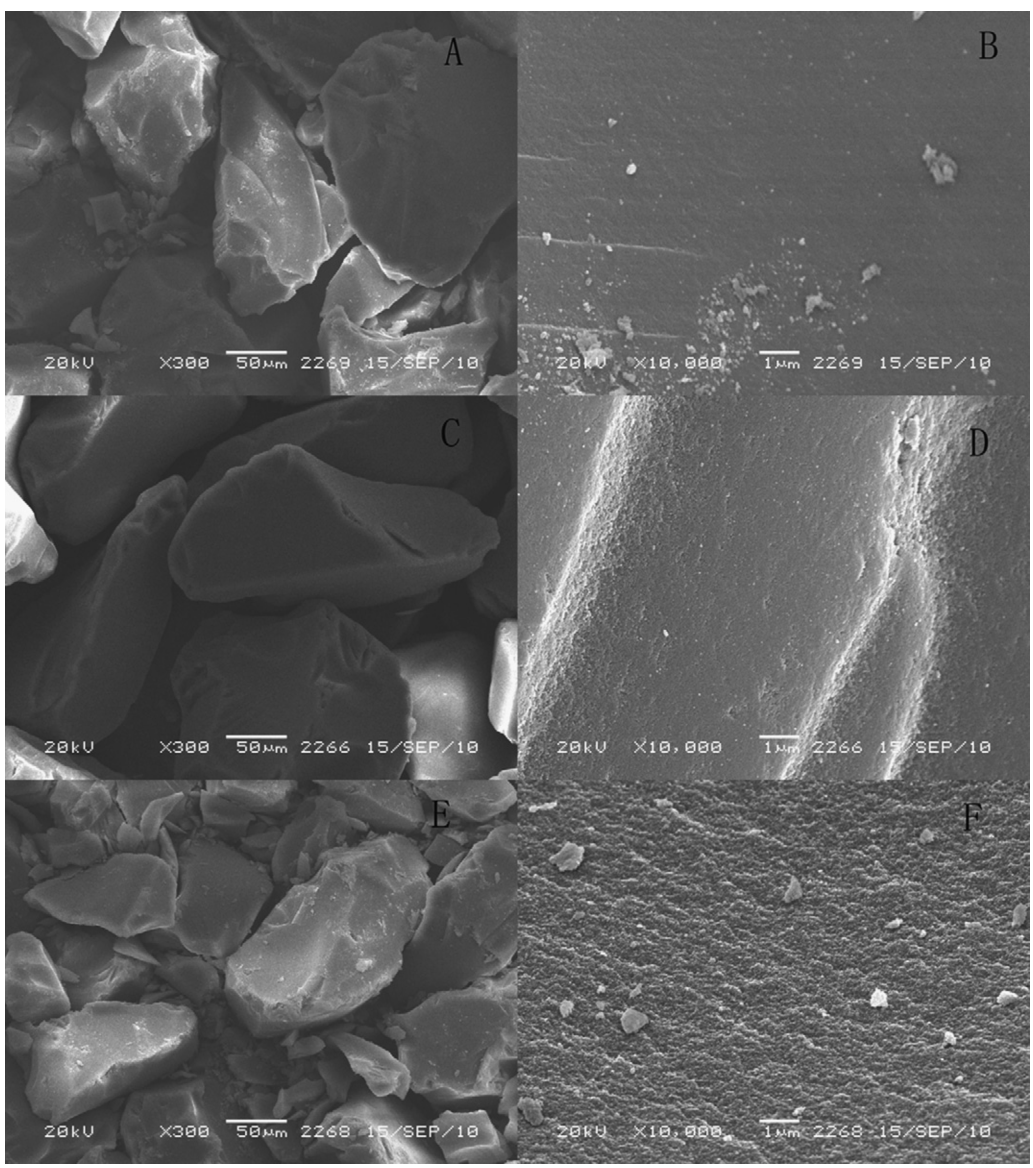

Fig. 4. SEM images of the activated silica gel (A and B), Si-Cl (C and D), Si-DTC (E and F).

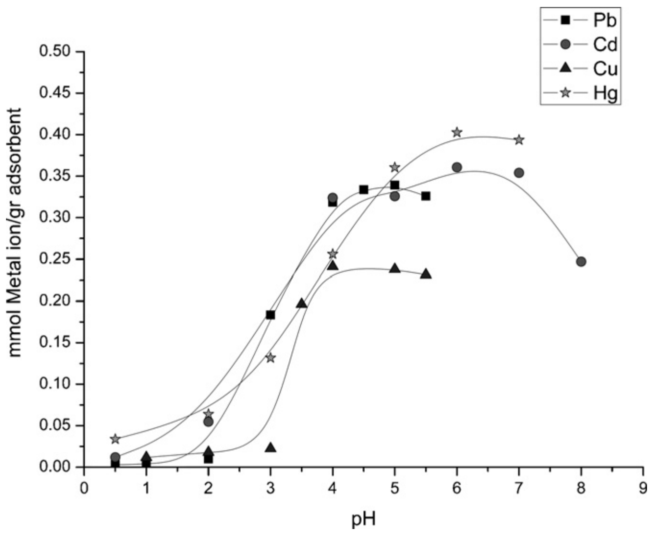

Fig. 5. The effect of pH on the adsorption of Pb(II), Cd(II), Cu(II) and Hg(II) metal ions. [(■) Pb(II)] C_0 = 200 mg L^{-1}; [(●) Cd(II)] C_0 = 100 mg L^{-1}; [(▲) Cu(II)] C_0 = 40 mg L^{-1}; [(⋆) Hg(II)] C_0 = 200 mg L^{-1}; t = 60 min; m(Si-DTC) = 0.05 g; temperature = 25 °C.

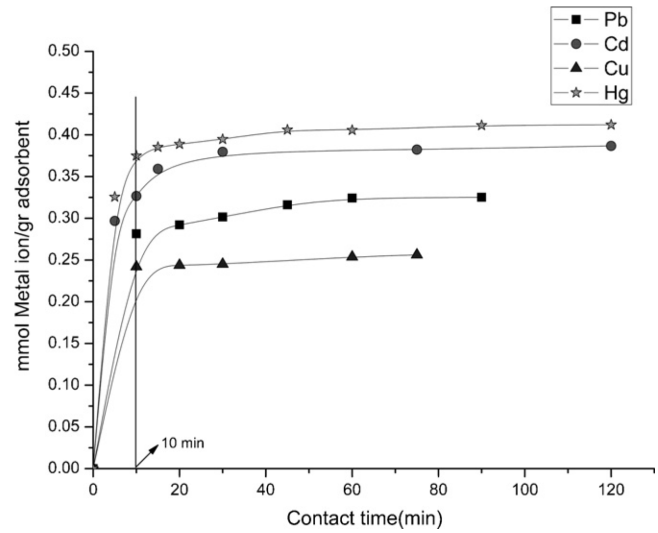

Fig. 6. Adsorption rates of heavy metal ions onto Si-DTC. [(■) Pb(II)] C_0=200 mg L^{-1}, pH 5.0; [(●) Cd(II)] C_0 = 100 mg L^{-1}, pH 7.0; [(▲) Cu(II)] C_0 = 40 mg L^{-1}, pH 5.0; [(⋆) Hg(II)] C_0 = 200 mg L^{-1}, pH 6.0; m(Si-DTC) = 0.20 g; temperature = 25 °C.

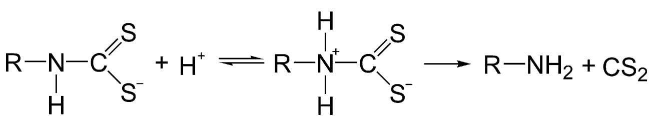

Scheme 4. The acid decomposition of dithiocarbamates.

3.1.4. Elemental analysis

Elemental analysis indicated 1.375% carbon, 28.96% nitrogen, 2.35% hydrogen and 1.10% sulfur in Si-DTC. It could be calculated that 1 g Si-DTC contained 0.17 mmol dithiocarbamate groups.

3.2. Adsorption behavior of Si-DTC

3.2.1. The effect of pH on adsorption

The medium pH value affected the surface charge of the adsorbent, the degree of ionization and speciation of adsorbate during reaction [25].Thus the adsorption of metal ions on Si-DTC was examined at the pH range of 0.5–8.0 and the results were presented in Fig. 5.

As shown in Fig. 5, a general increase in adsorption capacities with increasing pH of solution was observed. There was an abrupt increase at pH 3, which was close to the isoelectric point of the dithiocarbamate [26]. Below pH of 3, the H_3O^+ ions of higher concentration will compete with M(II) to seize the adsorption sites, and as a result, less adsorption capacities were observed at low pH. When the pH increased, the concentration of H_3O^+ ions decreased and the active adsorption sites mainly turned into dissociated forms, which resulted in the high affinity of adsorption sites towards the metal ions.

According to the literature [27], the dithiocarbamate compounds are generally unstable in acidic media and can be decomposed into the amine and carbon disulfide (presented in Scheme 4). And the dithiocarbamates began to decompose when the pH of the media was less than 4, and the decomposition rate reached maximum below pH of 2, which had been demonstrated in previous literatures [28,29]. All these indicate that during the pH range of 0.5–2.0 in our study, the dithiocarbamate groups were partially hydrolyzed, which also led to the poor adsorption capacities of Si-DTC at lower pH.

The optimum pH value at which the maximum metal uptake were obtained as 5.0, 7.0, 5.0 and 6.0 for Pb(II), Cd(II), Cu(II) and Hg (II), respectively. These optimum pH values were used for all subsequent experiments. However, Pb(II), Cd(II), Cu(II) and Hg(II) start to be precipitated as hydroxide at pH 6.0, 8.0, 6.0 and 7.0, respectively.

3.2.2. Adsorption dynamics

To determine an optimum contact time between the Si-DTC and heavy metal ion solutions, adsorption capacities of metal ions were measured as a function of contact time and the results were presented in Fig. 6.

As shown in Fig. 6, there was a rapid uptake kinetics and adsorption equilibria, which would be attained within 10 min. The adsorption equilibrium time of our study and some other dithiocarbamate based materials given in the literatures were summarized in Table 3. As listed in Table 3, the adsorption dynamics of Si-DTC

Table 3
Adsorption equilibrium time and adsorption capacities of some dithiocarbamate functionalized materials reported in the literatures.

Supporting material	Adsorption equilibrium time (min)	Adsorption capacities (mmol g^{-1})				Reference
		Pb	Cd	Cu	Hg	
Sporopollenin	30	0.45	0.06	0.27	–	[30]
Monosize polystyrene microspheres[a]	20	0.031	0.017	0.059	0.11	[16]
Macroreticular styrene-divinylbenzene copolymer	20	0.11	–	–	0.55	[31]
MCM-41-[N-(2-aminoethyl) dithiocarbamate]	90	0.018	0.013	0.032	–	[32]
Polymer/organosmectite	60/15	0.34	0.28	–	0.038	[33,34]
Silica (present study)	10	0.34	0.36	0.32	0.40	–

[a] Adsorption capacities in the presence of the heavy metals.

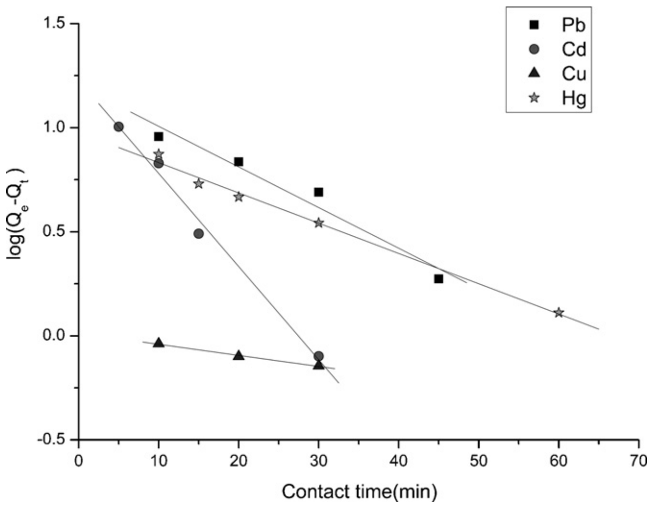

Fig. 7. Lagergren's pseudo-first-order plots for heavy metal ions on Si-DTC. [(■) Pb(II)] $C_0 = 200\,mg\,L^{-1}$, pH 5.0; [(●) Cd(II)] $C_0 = 100\,mg\,L^{-1}$, pH 7.0; [(▲) Cu(II)] $C_0 = 40\,mg\,L^{-1}$, pH 5.0; [(⋆) Hg(II)] $C_0 = 200\,mg\,L^{-1}$, pH 6.0; m(Si-DTC) = 0.20 g; temperature = 25 °C.

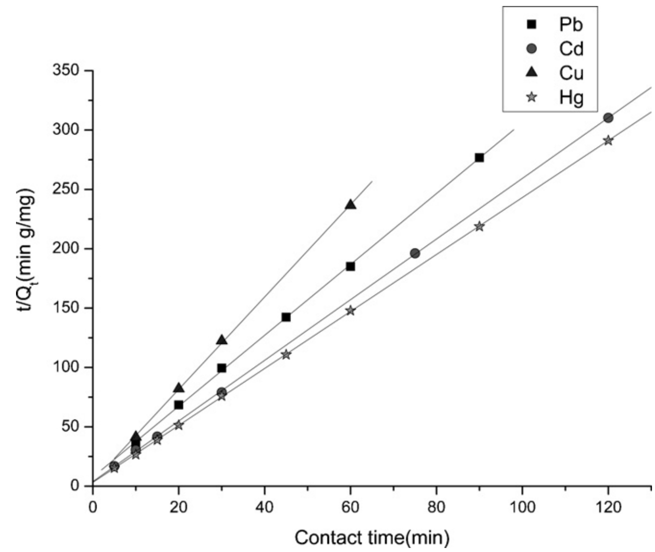

Fig. 8. Pseudo second-order plots for heavy metal ions on Si-DTC. [(■) Pb(II)] $C_0 = 200\,mg\,L^{-1}$, pH 5.0;[(●) Cd(II)] $C_0 = 100\,mg\,L^{-1}$, pH 7.0; [(▲) Cu(II)] $C_0 = 40\,mg\,L^{-1}$, pH 5.0;[(⋆) Hg(II)] $C_0 = 200\,mg\,L^{-1}$, pH 6.0; m(Si-DTC) = 0.20 g; temperature = 25 °C.

were much faster than the other dithiocarbamate functionalized adsorbents reported in the literatures [30,16,31–34]. Probably the fast adsorption of heavy metal ions onto Si-DTC could be ascribed to the good hydrophilicity of the silica matrix and the prominent chelate capacity of dithiocarbamate towards heavy metal ions. To ensure the equilibrium condition was achieved, the contact time of 60 min was chosen in the subsequent experiments.

In order to interpret the kinetic characteristics of metal adsorption processes, Lagergren first-order equation and pseudo-second-order equation model were used to evaluate experimental data.

The linearized form of the first-order rate equation by Lagergren and Svenska [35] is given as:

$$\log(Q_e - Q_t) = \log\, Q_e - \left(\frac{k_1 t}{2.303}\right), \quad (2)$$

where Q_e and Q_t are the amounts of the metal ions adsorbed ($mg\,g^{-1}$) at equilibrium and at contact time t (min), respectively, k_1 (min^{-1}) is the rate constant. The plots of $\log(Q_e - Q_t)$ versus t were depicted in Fig. 7 and the rate constants (k_1) and theoretical equilibrium adsorption capacities, Q_e (theor.) were presented in Table 4.

The experimental data were also fitted by the pseudo-second-order kinetic model which was given with the equation below [36]:

$$\frac{t}{Q_t} = \frac{1}{k_2 Q_e^2} + \left(\frac{1}{Q_e}\right) t, \quad (3)$$

where k_2 ($g\,mg^{-1}\,min^{-1}$) is the rate constant of pseudo second-order adsorption reaction. The plots of t/Q_t versus t were shown in Fig. 8 and the rate constants (k_2) and theoretical equilibrium adsorption capacities, Q_e (theor.) were presented in Table 4.

From Table 4, the calculated equilibrium adsorption capacities, Q_e (theor.) of the pseudo-first-order kinetic model were not in accordance with the experimental adsorption capacities Q_e (exp.). Furthermore, linear correlation coefficients of the plots for all the four metal ions were not good. Therefore, it suggested that the adsorption of Pb(II), Cd(II), Cu(II) and Hg(II) onto Si-DTC cannot be described by first-order kinetic reaction. As to the pseudo-second-order model, the correlation coefficients for the slopes were superior to 0.999 in all the systems and the theoretical Q_e values were close to the experimental Q_e values. It was possible to suggest that the adsorption of Pb(II), Cd(II), Cu(II) and Hg(II) onto Si-DTC followed a second-order type reaction kinetics. The pseudo-second-order model is based on the assumption that the rate-determining step may be a chemical adsorption involving valence forces through sharing or exchanging of electrons between adsorbent and adsorbate [37].

3.2.3. Adsorption isotherms

The effect of initial concentrations on metal ion adsorption was investigated by varying the initial concentrations of the metal ions at optimum pH value and 60 min of equilibration time. The obtained results were presented in Fig. 9.

From Fig. 9, the higher is the initial concentration of the metal ion, the larger is the amount of the metal ion taken up. This increase in loading capacity of the adsorbent with relation to the metal ions concentration can be explained with the high driving force for mass transfer [38]. The maximum adsorption capacity could reach to $0.34\,mmol\,g^{-1}$, $0.36\,mmol\,g^{-1}$, $0.32\,mmol\,g^{-1}$ and $0.40\,mmol\,g^{-1}$ for Pb(II), Cd(II), Cu(II) and Hg(II), respectively, in the range of the experimental concentrations. The adsorption capacities of our study and some other dithiocarbamate based materials given in

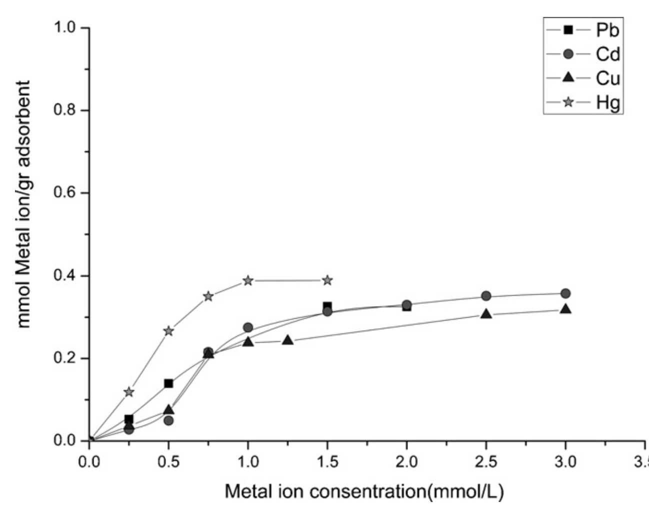

Fig. 9. Effect of initial concentration on heavy metal adsorption for Si-DTC. [(■) Pb(II)] pH 5.0; [(●) Cd(II)] pH 7.0; [(▲) Cu(II)] pH 5.0; [(⋆) Hg(II)] pH 6.0 ; m(Si-DTC) = 0.05 g; temperature = 25 °C.

Table 4
First-order, second-order rate constants.

Metal	First-order rate constants				Second-order rate constants		
	Q_e (exp) (mg g^{-1})	k_1 (min^{-1})	Q_e (theor.) (mg g^{-1})	R^2	k_2 (g mg^{-1} min^{-1})	Q_e (theor.) (mg g^{-1})	R^2
Pb	67.39	0.0450	15.92	0.9587	0.000027	69.40	0.9996
Cd	43.47	0.1031	16.90	0.9901	0.000133	44.00	0.9999
Cu	16.40	0.0365	1.604	0.9314	0.000960	16.45	0.9997
Hg	82.71	0.0335	9.492	0.9913	0.000044	83.64	0.9999

the literature were summarized in Table 3. As can be seen from Table 3, these adsorption capacities of our materials are comparable to some other dithiocarbamate functionalized adsorbents reported before.

The adsorption data for heavy metal ions were analyzed by fitting the Langmuir, Freundlich and D–R adsorption isotherm models.

The Langmuir isotherm model assumes a monolayer adsorption which takes place at specific homogeneous sites within the adsorbent and all the adsorption sites are energetically identical. In this model, a M(II) monolayer is formed on a modified adsorbent with a metal complex formation [39]. Linearized form of the Langmuir equation was given by the following equation [40]:

$$\frac{1}{Q_e} = \frac{1}{Q^0} + \frac{1}{bQ^0C_e}, \tag{4}$$

where Q_e is the amount of metal ion adsorbed on the adsorbent (mmol g^{-1}), C_e is the equilibrium metal ion concentration in the solution (mmol L^{-1}), Q^0 represents a practical limiting adsorption capacity when the surface of adsorbent is completely covered with adsorbate and b is the Langmuir adsorption constant (L mmol^{-1}). The plots of $1/Q_e$ versus $1/C_e$ were shown in Fig. 10 and the values of Q^0 and b were presented in Table 5.

The Freundlich model assumes a heterogeneous adsorption surface with sites having different adsorption energies. Linearized form of the Freundlich equation was given by the following equation [41]:

$$\log Q_e = \log K_F + \frac{1}{n} \log C_e, \tag{5}$$

where Q_e is the equilibrium metal ion concentration on adsorbent (mmol g^{-1}), C_e is the equilibrium concentration of the metal ion (mmol L^{-1}), K_F is the Freundlich constant (mmol g^{-1}) which indicates the adsorption capacity and represents the strength of the adsorptive bond and n is the heterogeneity factor which represents the bond distribution. The plots of $\log Q_e$ versus $\log C_e$ were shown in Fig. 11 and the values of K_F and n were presented in Table 5.

The D–R isotherm is more general than the Langmuir isotherm, because it does not assume a homogeneous surface or constant adsorption potential. The equilibrium data were also examined by the Dubinin–Radushkevich (D–R) model to determine the nature of adsorption processes whether it is physical or chemical [42].The D–R isotherm is given with the following Eq. (6) [43]:

$$Q = Q_m \exp(-k\varepsilon^2), \tag{6}$$

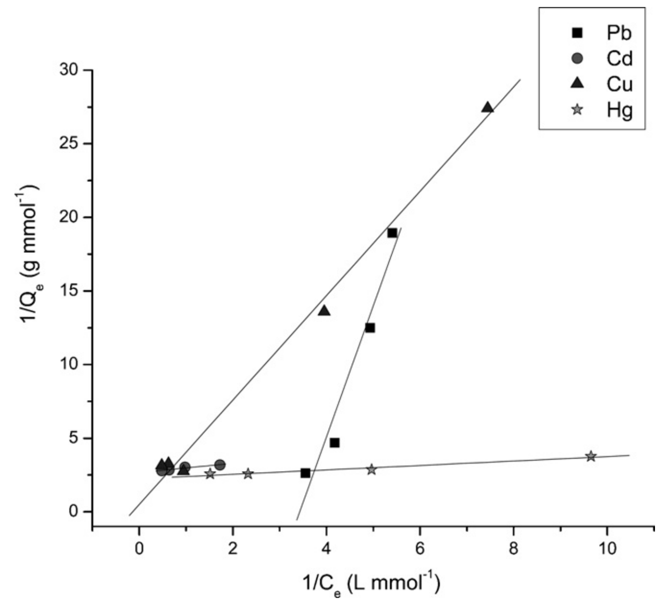

Fig. 10. Langmuir isotherm plots for heavy metal ions on Si-DTC. [(■) Pb(II)] pH 5.0; [(●) Cd(II)] pH 7.0; [(▲) Cu(II)] pH 5.0; [(⋆) Hg(II)] pH 6.0 ; m(Si-DTC) = 0.05 g; temperature = 25 °C.

and linearized form of the equation was given as Eq. (7):

$$\ln Q = \ln Q_m - k\varepsilon^2, \tag{7}$$

where Q is the amount of metal ion adsorbed per unit weight of adsorbent (mol g^{-1}), k is a constant related to the adsorption energy (mol^2 kJ^{-2}) and Q_m is the maximum adsorption capacity (mol g^{-1}), ε is the Polanyi potential (J mol^{-1}) that can be written as:

$$\varepsilon = RT \ln\left(1 + \frac{1}{C_e}\right). \tag{8}$$

The plots of $\ln Q$ versus ε^2 were shown in Fig. 12 and the values of Q_m and k were presented in Table 5.

Know from Table 5, the adsorption processes could not be described by the Langmuir adsorption isotherm model as negative values of b and Q^0 were obtained and the linear correlation coefficients (R^2) of the plots for all the four metal ions were not good. The R^2 values were in the range 0.85–0.99 indicating that the adsorption processes did not fit well with the Freundlich model. Consequently, the D–R isotherm model fitted best to the experimental data when the R^2 values were compared and the maximum adsorption Q_m values calculated from the experimental data were in good accordance

Table 5
Langmuir, Freundlich and D–R isotherm constants.

Metal	Langmuir isotherms parameters			Freundlich isotherms parameters			D–R isotherms parameters		
	Q^0 (mmol g^{-1})	b (L mmol^{-1})	R^2	K_F (mmol g^{-1})	n	R^2	Q_m (mmol g^{-1}	k (mol^2 kJ^{-2})	R^2
Pb	−0.0327	−3.4313	0.9489	0.3725	0.9656	0.9207	0.3635	0.00046	0.9960
Cd	0.3753	8.4767	0.9471	0.3319	9.3703	0.9818	0.3609	0.00012	0.9995
Cu	2.0133	0.1400	0.9924	0.1901	1.2220	0.9952	0.3144	0.00003	0.9998
Hg	0.4455	14.9447	0.9659	0.2806	4.9576	0.8553	0.3893	0.00278	0.9974

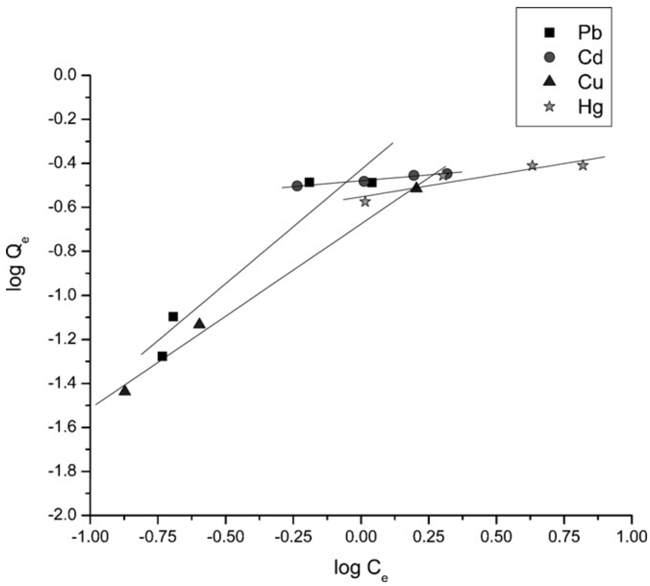

Fig. 11. Freundlich isotherm plots for heavy metal ions on Si-DTC. [(■) Pb(II)] pH 5.0; [(●) Cd(II)] pH 7.0; [(▲) Cu(II)] pH 5.0; [(⋆) Hg(II)] pH 6.0 ; m(Si-DTC) = 0.05 g; temperature = 25 °C.

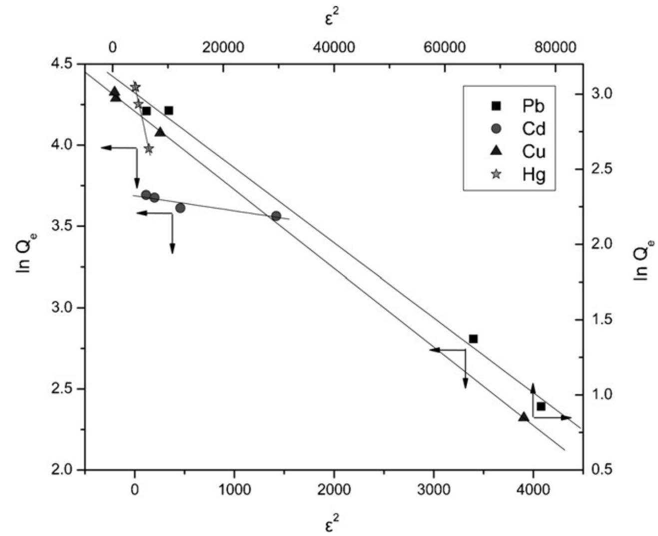

Fig. 12. D–R isotherm plots for heavy metal ions on Si-DTC. [(■) Pb(II)] pH 5.0; [(●) Cd(II)] pH 7.0; [(▲) Cu(II)] pH 5.0; [(⋆) Hg(II)] pH 6.0 ; m(Si-DTC) = 0.05 g; temperature = 25 °C.

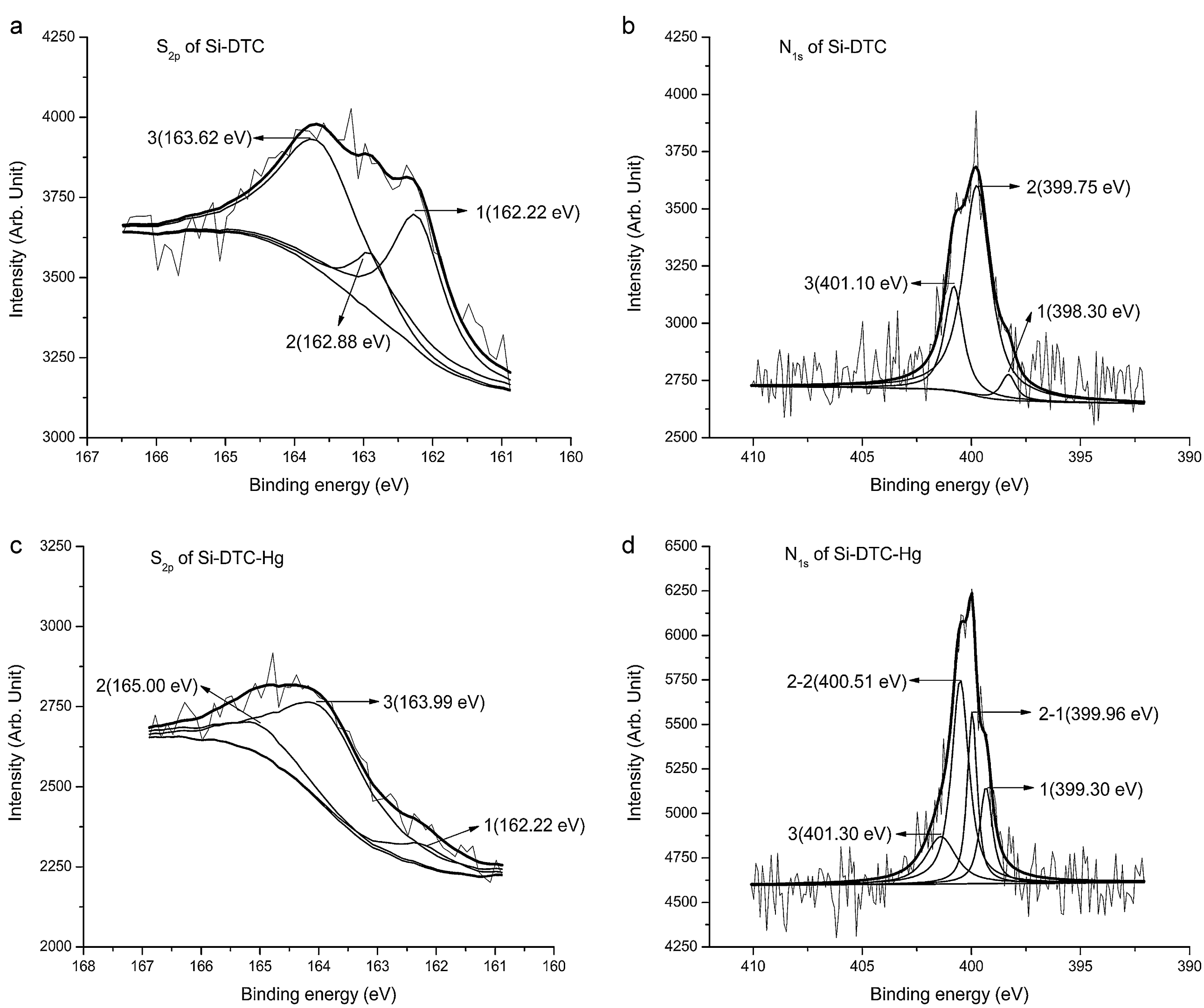

Fig. 13. The high-resolution core-level spectra of N_{1s} and S_{2p} for Si-DTC and Si-DTC-Hg.

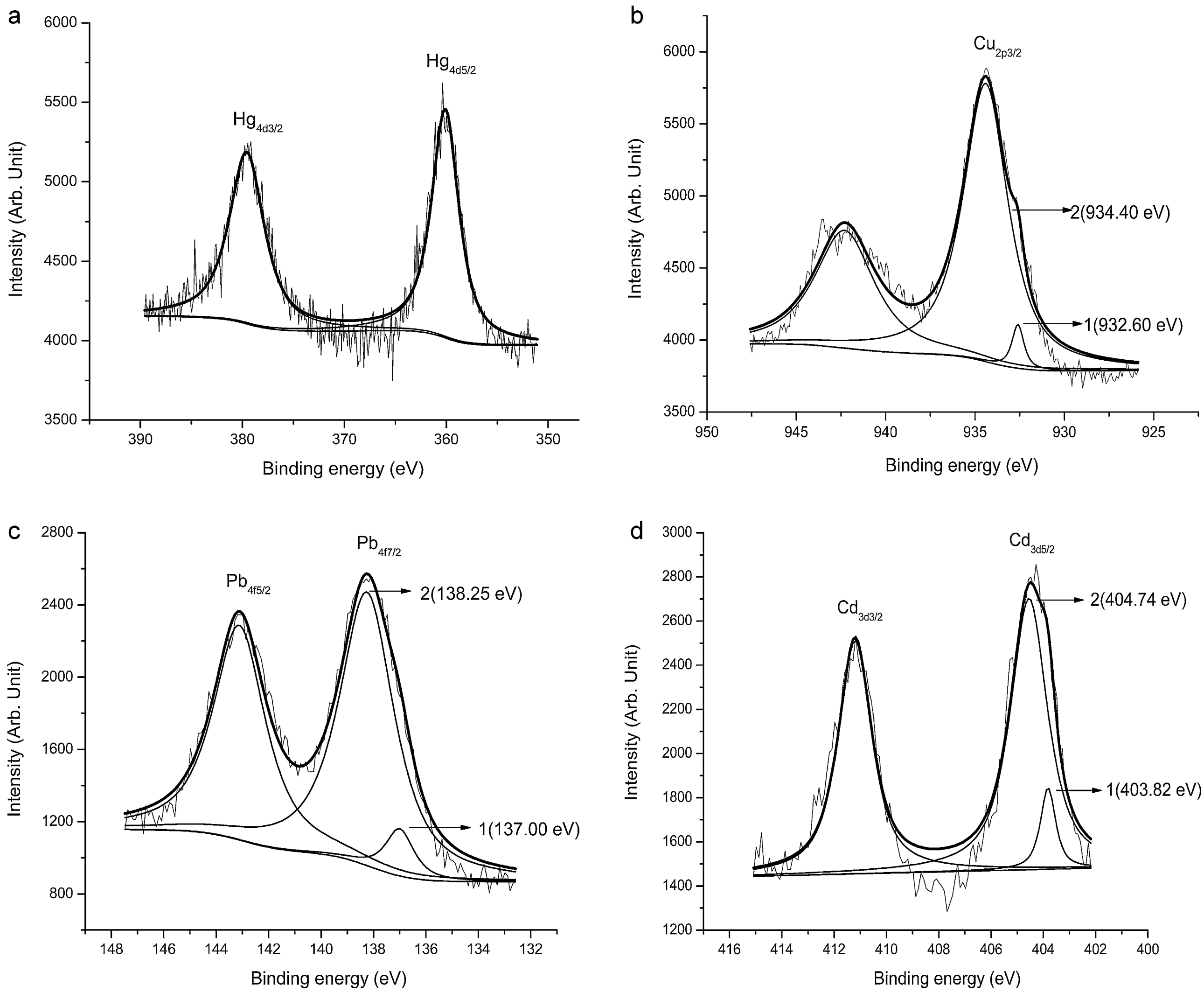

Fig. 14. The high-resolution core-level spectra of (a) Hg_{4d} in Si-DTC-Hg, (b) $Cu_{2p3/2}$ in Si-DTC-Cu, (c) $Pb_{4f7/2}$ in Si-DTC-Pb and (d) $Cd_{3d5/2}$ in Si-DTC-Cd.

with the experimental Q values. The Dubinin–Radushkevitch (D–R) equation was originally proposed as an empirical adaptation of the Polanyi adsorption potential theory. In our study, there appeared multihole structure on the surface of Si-DTC as shown in Fig. 4F, mainly because the microcorrosion of the silica matrix surface by the solution with a pH value of 9–10 during the synthesis of Si-DTC. Therefore, the adsorption of heavy metal ions onto the Si-DTC surface was pore-filling rather than layer-by-layer surface coverage, which was in correspondence with the postulate of the D–R equation [44].

To evaluate the nature of interaction between heavy metal ions and the binding sites, the mean free energy of adsorption (E) was calculated from the k values using the following equation [45]:

$$E = (2k)^{-\frac{1}{2}}. \tag{9}$$

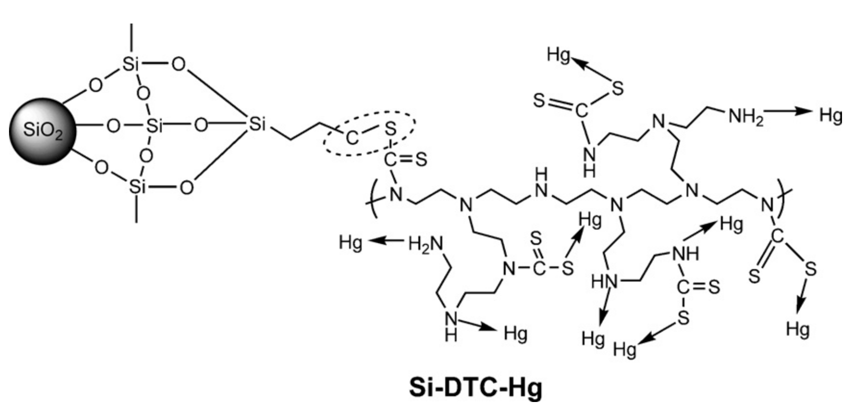

Scheme 5. The structure of Si-DTC-Hg.

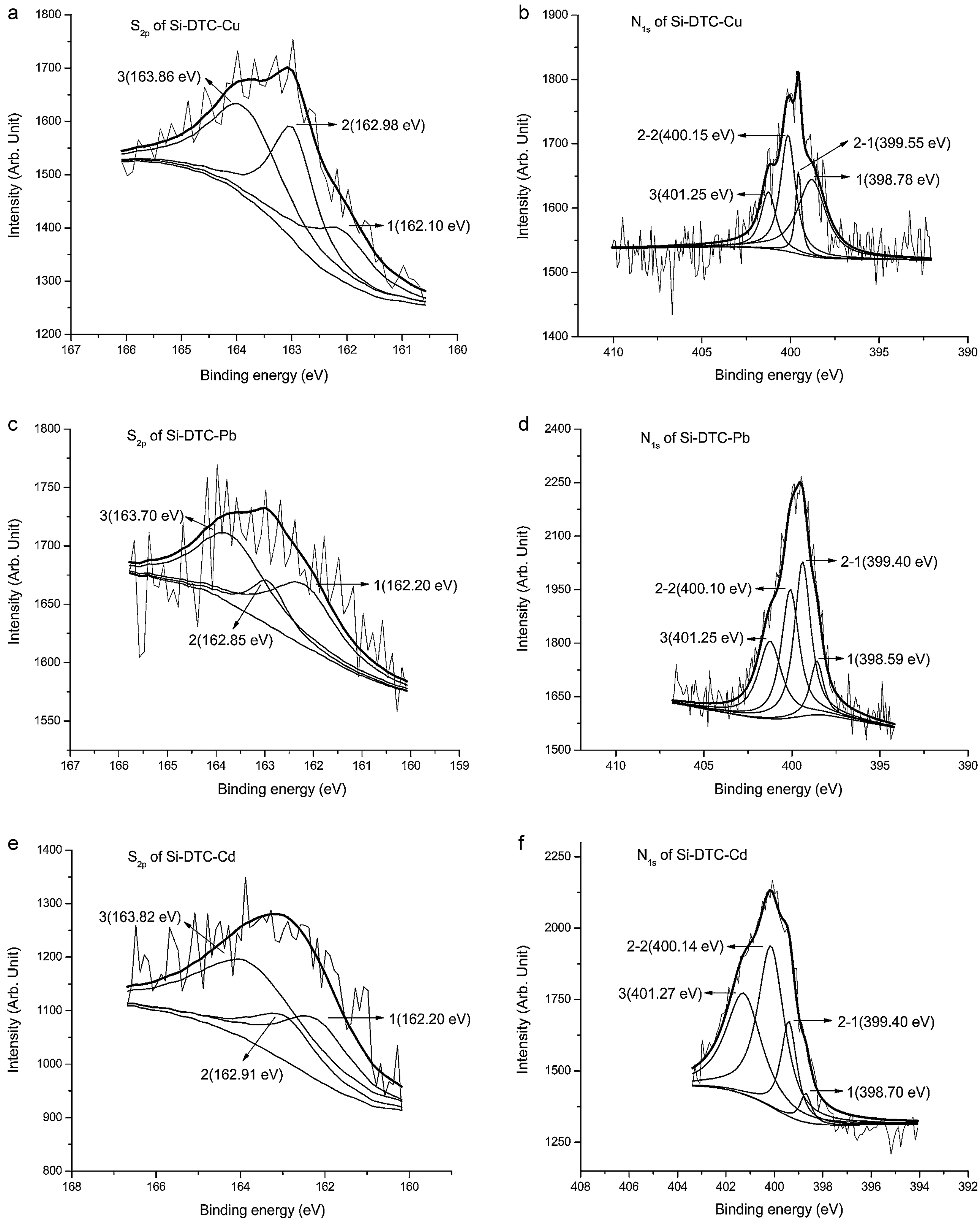

Fig. 15. The high-resolution core-level spectra of N_{1s} and S_{2p} for Si-DTC-Cu, Si-DTC-Pb and Si-DTC-Cd.

The values of E were found to be 32.96 kJ mol^{-1}, 64.55 kJ mol^{-1}, 129.10 kJ mol^{-1} and 13.41 kJ mol^{-1} for Pb(II), Cd(II), Cu(II) and Hg(II), respectively. The mean free energy of adsorption (E) per mole of the adsorbate is the energy required to transfer one mole of an adsorbate to the surface from infinity in solution [46]. The E value of Hg(II) is much smaller than the E values of Pb(II), Cd(II) and Cu(II), i.e., it needs much more energy to transfer Pb(II), Cd(II) and Cu(II) onto the surface of Si-DTC than Hg(II), which results in stronger adsorbing tendency of Hg(II) onto the surface of Si-DTC than that of Pb(II), Cd(II) and Cu(II), and this also indicates that the

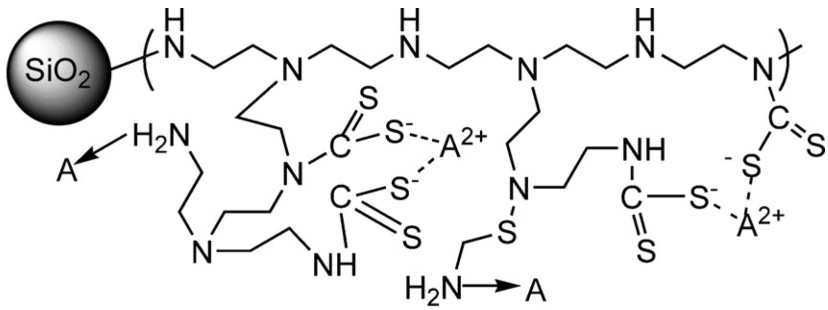

Si-DTC-A

Scheme 6. The structure of Si-DTC-A (A = Pb(II), Cd(II) or Cu(II))

adsorption mechanism of Hg(II) onto Si-DTC may be quite different from that of Pb(II), Cd(II) or Cu(II) onto Si-DTC. Moreover, the magnitude of *E* values indicates the adsorbing tendency of Si-DTC to heavy metal ions, which basically matches the adsorption capacities order in our study because the adsorption capacity of Hg(II) from Si-DTC is much higher than that of Pb(II), Cd(II) and Cu(II).

3.2.4. Adsorption mechanism of Pb(II), Cd(II), Cu(II) and Hg(II) onto Si-DTC

In order to clarify the adsorption mechanism of Pb(II), Cd(II), Cu(II) and Hg(II) onto Si-DTC, the XPS analyses for Si-DTC and M(II) loaded Si-DTC (abbreviated as Si-DTC-M) were done.

Table 6
Thermodynamic parameters for the adsorption of Pb(II), Cd(II), Cu(II) and Hg(II) on Si-DTC.

Metal	C_0 (mg L^{-1})	ΔH° (kJ mol^{-1})	ΔS° (J K^{-1} mol^{-1})	T (K)	ΔG° (kJ mol^{-1})	R^2
				303	−18.50	
				308	−18.84	
		1.69	66.46	313	−19.17	0.9913
				318	−19.50	
				323	−19.83	
Pb	200			328	−20.16	
				333	−21.84	
				338	−22.52	
		23.46	135.96	343	−23.20	0.9945
				348	−23.88	
				353	−24.56	
				303	−17.82	
				308	−18.15	
				313	−18.47	
		1.72	64.47	318	−18.79	0.9928
				323	−19.11	
Cd	100			328	−19.44	
				333	−21.17	
				338	−21.84	
				343	−22.52	0.9913
		23.83	135.07	348	−23.19	
				353	−23.87	
				303	−18.70	
				308	−19.03	
				313	−19.36	
		1.34	66.10	318	−19.69	0.9933
				323	−20.03	
Cu	60			328	−20.36	
				333	−22.27	
				338	−22.96	
				343	−23.66	
		24.03	138.96	348	−24.35	0.9926
				353	−25.05	
				303	−24.54	
				308	−25.02	
				313	−25.49	0.9933
		4.40	95.45	318	−25.97	
				323	−26.45	
Hg	200			328	−26.93	
				333	−27.54	
				338	−28.12	
				343	−28.71	0.9908
		11.31	116.60	348	−29.29	
				353	−29.87	

3.2.4.1. The XPS results of Si-DTC and Si-DTC-Hg. The high-resolution core-level spectra of S_{2p} and N_{1s} of Si-DTC and Si-DTC-Hg resolved into individual component peaks were shown in Fig. 13. The S_{2p} binding energies of C–S bond of dithiocarbamate group in Si-DTC and Si-DTC-Hg were 162.88 eV (peak 2 in Fig. 13a) and 165.00 eV (peak 2 in Fig. 13c), respectively, i.e., the S_{2p} binding energy of C–S bond of dithiocarbamate groups in Si-DTC-Hg was much higher than that in Si-DTC, which results from the donation of the electrons from S atoms of C–S bonds of dithiocarbamate groups to Hg(II) [47]. The peak 3 at 163.62 eV in Fig. 13a and peak 3 at 163.99 eV Fig. 13c were attributed to a new C–S bond [48] in Si-DTC-1(presented in Scheme 3) and this new C–S bond in Si-DTC-Hg (presented in Scheme 5) without the complexing formation between Hg(II), respectively. The S_{2p} binding energies of the C=S bond of dithiocarbamate groups [49] in Si-DTC (peak 1 in Fig. 13a) and Si-DTC-Hg (peak 1 in Fig. 13c) were both 162.22 eV, which indicates no chelating bond is formed between Hg(II) and the C=S bond.

The N_{1s} binding energies of N–CS_2 bond in Si-DTC and in Si-DTC-Hg were 398.30 eV (peak 1 in Fig. 13b) and 399.30 eV (peak 1 in Fig. 13d), respectively, i.e., the N_{1s} binding energy of N–CS_2 bond in Si-DTC-Hg was higher than that in Si-DTC. This is because of the chelating formation between Hg(II) and the N atom of dithiocarbamate group [47], which results in the transfer of electrons from N atom of dithiocarbamate group to Hg(II). The peak 2 at 399.75 eV in Fig. 13b corresponded to the –NH/–NH_2 groups, which had not been subjected to dithiocarbamation in Si-DTC. The peak 2-2 at 400.51 eV in Fig. 13d corresponded to the –NH/–NH_2 groups which forms complexes with Hg(II) in Si-DTC-Hg, i.e., the N_{1s} binding energy of a portion of –NH/–NH_2 groups in Si-DTC increased about 0.8 eV after the adsorption of Hg(II), which results from the donation of the lone pair of electrons of N atom to the shared bond between the N atom of –NH/–NH_2 groups and Hg(II), and as a consequence, the electron cloud density of this N atom decreased [50,51]. The N_{1s} binding energies of –NR_2 in Si-DTC and in Si-DTC-Hg were 401.10 eV (peak 3 in Fig. 13b) and 401.30 eV (peak 3 in Fig. 13d) in Si-DTC-Hg [52], respectively, i.e., there was no obvious change of N_{1s} binding energies of –NR_2 after the adsorption for Hg(II), which indicates that there was no or little chelating interaction between tertiary amines and Hg(II).

Since the spectra of Hg_{4f} overlaps with that of Si_{2p}, the signal of Hg_{4d} was presented in Fig. 14a to investigate the adsorption of Hg(II) on Si-DTC. The binding energy of $Hg_{4d5/2}$ and $Hg_{4d3/2}$ both revealed single peak around 360.10 eV and 378.30 eV, respectively, which indicates that Hg(II) was adsorbed only through the chelating binding between Hg(II) and sulfur or nitrogen [53].

3.2.4.2. The XPS results of Si-DTC-Cu, Si-DTC-Pb and Si-DTC-Cd. The high-resolution core-level spectra of S_{2p} and N_{1s} of Si-DTC-Cu, Si-DTC-Pb and Si-DTC-Cd resolved into individual component peaks were shown in Fig. 15. The S_{2p} binding energies of C=S bond of dithiocarbamate groups (peak 2 in Fig. 15a), C–S bond of dithiocarbamate group (peak 2 in Fig. 15a) and a new C–S bond (peak 3 in Fig. 15a) in Si-DTC-1, were 162.10 eV, 162.98 eV and 163.86 eV, respectively, i.e., the S_{2p} binding energies of all these three kinds of bonds in Si-DTC-Cu were almost the same with those in Si-DTC. From Fig. 15b, the N_{1s} binding energies of N–CS_2 bond (peak 1), –NH/–NH_2 groups (peak 2-1/peak 2-2) and –NR_2 (peak 3) in Si-DTC-Cu, were 398.78 eV, 399.55 eV/400.15 eV and 401.25 eV, respectively. According to the analysis results for N_{1s} binding energies of Si-DTC and Si-DTC-Hg, these results indicate that the –NH/–NH_2 groups were also formed as complexes with Cu(II) in Si-DTC-Cu.

The S_{2p} and N_{1s} results of Si-DTC-Pb and Si-DTC-Cd (presented in Fig. 15c–f) were almost the same with those of Si-DTC-Cu, and this shows that the adsorption mechanisms of Si-DTC for Pb(II), Cd(II) or Cu(II) were the same.

It seemed no chemical combination between Cu(II), Pb(II) or Cd(II) and the C–S bond of dithiocarbamate groups. Nevertheless, the high-resolution core-level spectra of $Cu_{2p3/2}$, $Pb_{4f7/2}$ and $Cd_{3d5/2}$ reveal notable phenomena in Fig. 14b–d. Fig. 14b shows the main peak of $Cu_{2p3/2}$ around 934.40 eV, along with its weaker satellite peak around 942.78 eV [54]. The peak of $Cu_{2p3/2}$ was resolved into two component peaks. Peak 1 at 932.60 eV was characteristic of the complexation which was formed between –NH/–NH_2 groups and Cu(II) [55]. Peak 2 at 934.30 eV corresponded to the $Cu_{2p3/2}$ electron binding energies of the cupric forms [56], which suggests that Cu(II) was seized in cupric forms by the dissociated dithiocarbamate sites at the same time.

The spectral decomposition results of $Pb_{4f7/2}$ in Fig. 14c and $Cd_{3d5/2}$ in Fig. 14d also show two valence states, respectively, one is of divalent ion form and another of metal-amine complexes [55,57–59], which were similar to $Cu_{2p3/2}$. It also suggests that the adsorption mechanisms of Si-DTC for Pb(II) or Cd(II) were in accordance with that for Cu(II).

3.2.4.3. The differences of adsorption mechanisms between Pb(II), Cd(II), Cu(II) or Hg(II) onto Si-DTC. The N_{1s} binding energy results for Si-DTC and Si-DTC-M indicate that there were a portion of the –NH/–NH_2 groups conformed coordination with all of the four heavy metal ions, that's the reason why adsorption amounts of Si-DTC to metal ions were much higher than the content of dithiocarbamate groups attached to silica matrix.

As discussed in Sections 3.2.4.1 and 3.2.4.2, the adsorption mechanism of Hg(II) (presented in Scheme 5) is quite different from that of Pb(II), Cd(II) or Cu(II) (presented in Scheme 6). Besides the –NH/–NH_2 groups, the N atom of N–CS_2 and the S atom of the C–S bond in dithiocarbamate groups were also coordinated to the Hg(II), while no chelating reactions for Pb(II), Cd(II) or Cu(II) took place with the N atom of N–CS_2 and the S atom of the C–S bond. However, the XPS results of $Cu_{2p3/2}$, $Pb_{4f7/2}$ and $Cd_{3d5/2}$ suggest that a portion of Pb(II), Cd(II) and Cu(II) were adsorbed in a divalent ion form by the dithiocarbamate anions, i.e., there were also chemical bonds which were formed between Pb(II), Cd(II) or Cu(II) with the C–S bond of dithiocarbamate groups.

Moreover, the FI-IR results of MDTC, DTC-Pb, DTC-Cd, DTC-Cu and DTC-Hg in Section 3.1.1 also evidenced the differences of the adsorption mechanisms. As shown in Table 1, the order of absorption redshift for the C–S bond of dithiocarbamate group was DTC-Hg > DTC-Cd > DTC-Pb > DTC-Cu. The combination between Hg(II) and the C–S bond was of strong covalent properties, which leads to the most prominent shift of the adsorption frequency. Meanwhile, the chemical bindings of Pb(II), Cd(II) or Cu(II) to the dithiocarbamate anions had weak tendencies of sharing electrons, which results in the relatively small variation of the C–S bond adsorption frequencies. The stretching vibration of N–CS_2 bond of MDTC at 1453 cm^{-1} revealed considerable double bond characteristics, because the stretching mode of the single C–N bond is shortened under the influence of the polar ionic bond of C^+–S^- [47,60]. From Table 1, the stretching vibration frequencies of N–CS_2 bond of DTC-Pb, DTC-Cd and DTC-Cu shifted to higher frequencies comparing with MDCT, it is because the chemical bindings of Pb(II), Cd(II) or Cu(II) to the C–S bond of dithiocarbamate group produce the effect of electrostatic induction, which enhances the double bond characteristics of the N–CS_2 bond. As for DTC-Hg, the N atom of N–CS_2 bond and the S atom of the C–S bond in dithiocarbamate groups both have the tendencies to transfer electrons to Hg(II), which counteracts the tendency of the electron cloud dispersing to the two sides of N–CS_2 bond, as a result, the stretching vibration of N–CS_2 bond of DTC-Hg does not change, and is almost the same with MDTC.

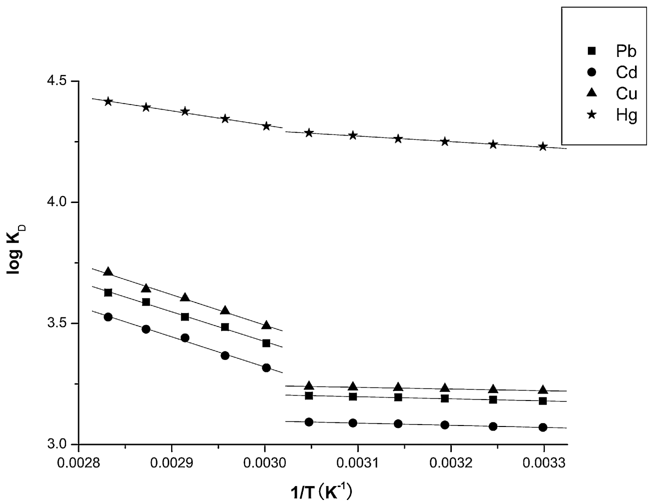

Fig. 16. The $\log K_D{}^{-1}/T$ graphs for the adsorption of heavy metal ions on Si-DTC. [(■) Pb(II)] $C_0 = 200\,\mathrm{mg\,L^{-1}}$, pH 5.0; [(●) Cd(II)] $C_0 = 100\,\mathrm{mg\,L^{-1}}$, pH 7.0; [(▲)Cu(II)] $C_0 = 60\,\mathrm{mg\,L^{-1}}$, pH 5.0; [(⋆) Hg(II)] $C_0 = 200\,\mathrm{mg\,L^{-1}}$, pH 6.0; m(Si-DTC) = 0.05 g; t = 60 min.

3.2.5. *Adsorption thermodynamics*

The effect of temperature on the adsorption of heavy metal ions onto Si-DTC was given from the plots and curves of the distribution coefficient K_d values versus adsorption temperatures in Fig. 16.

It can be found in Fig. 16 that K_d increased with temperature increasing, a certification of the endothermic adsorption nature. Thermodynamic parameters including free energy change (ΔG^o), enthalpy change (ΔH^o) and entropy change (ΔS^o) were calculated according to Eqs. (10)–(12). The Gibbs free energy change of the process was related to the distribution coefficient (K_d) in the linearized form of Eq. (10):

$$\Delta G^o = -RT \ln K_d \tag{10}$$

$$\Delta G^o = \Delta H^o - T\Delta S^o \tag{11}$$

$$\log K_d = \frac{\Delta S^o}{2.303R} - \frac{\Delta H^o}{2.303RT}, \tag{12}$$

where K_d is the distribution coefficient ($\mathrm{mL\,g^{-1}}$), and R is the gas constant ($8.314\,\mathrm{J\,mol^{-1}\,K^{-1}}$). The calculated values of thermodynamic parameters were listed in Table 6.

As shown in Table 6, the values of ΔG^o were negative at all temperatures, confirming that the adsorption of heavy metal ions onto Si-DTC was spontaneous and thermodynamically favorable. The increase in absolute value of $-\Delta G^o$ as temperature rising indicates that the adsorption process of metal ions on Si-DTC becomes more favorable at higher temperature. The positive values of ΔS^o suggest the randomness at the solid-solution interface increases during the adsorption of heavy metal ions on Si-DTC.

The enthalpy changes ΔH^o were positive at all temperatures represented the endothermic natures of adsorption processes and the heat maybe consumed to transfer the heavy metal ions from aqueous solution onto Si-DTC. Although there are no certain criteria related to the ΔH^o values that define the adsorption type, the heat of adsorption values between $20.9\,\mathrm{kJ\,mol^{-1}}$ and $418.4\,\mathrm{kJ\,mol^{-1}}$ are frequently assumed as the comparable values for chemical adsorption processes [61]. Known from Table 6, ΔH^o values were $1.69\,\mathrm{kJ\,mol^{-1}}$, $1.72\,\mathrm{kJ\,mol^{-1}}$, $1.34\,\mathrm{kJ\,mol^{-1}}$ and $4.40\,\mathrm{kJ\,mol^{-1}}$ for Pb(II), Cd(II), Cu(II) and Hg(II), respectively, at the range of 303K–328K. We hypothesized that in the range of 303K–328K, the transportation of heavy metal ions from aqueous solution onto the surface of Si-DTC was improved by the increasing temperature, which reveals a physical nature of the adsorption process. And the ΔH^o values were $23.46\,\mathrm{kJ\,mol^{-1}}$, $23.83\,\mathrm{kJ\,mol^{-1}}$, $24.03\,\mathrm{kJ\,mol^{-1}}$ and $11.31\,\mathrm{kJ\,mol^{-1}}$ for Pb(II), Cd(II), Cu(II) and Hg(II), respectively, in the range of 333K–353K. This is probably because in the range of 333K–353K, the transportation of heavy metal ions was not appreciably improved by the increasing temperature, but the chelating reactivity of Si-DTC for heavy metal ions was promoted by the higher temperature. In this way, the chemical reaction became the leading factor during the adsorption process.

4. Conclusions

In the presented study, a new procedure for the efficient synthesis of silica-supported dithiocarbamate (Si-DTC) has been developed which observably improved the adsorption capacities of dithiocarbamate adsorbent and the properties of this adsorbent have been examined. The adsorption behavior of heavy metal ions by Si-DTC is pH-dependent and the decomposition of dithiocarbamate in acid media leads to the poor adsorption capacities of Si-DTC at lower pH.

The adsorption process for the heavy metal ions for Si-DTC can be explained with pseudo second-order type kinetic model, which is based on the assumption that the rate-determining step is a chemical adsorption. The adsorption of all the metal ions on Si-DTC could be expressed by D–R type adsorption isotherms, which shows the non-homogenous characteristics of the adsorption sites on the adsorbent. Chelating interactions are accompanied by an increase in entropy and exhibit endothermic enthalpy values. The dithiocarbamate groups and the amino groups in Si-DTC both take part in the adsorption process for M(II) from aqueous solutions but the adsorption mechanism of Hg(II) onto Si-DTC is quite different from that of Pb(II), Cd(II) or Cu(II) onto Si-DTC, which is testified by the XPS and FT-IR results.

Acknowledgements

The authors are grateful to the National Basic Research Program of China (973 Project) (No. 2007CB613601), the College Student Innovation Experiment Program of Central South University (No. LC09096) and the Program for New Century Excellent Talents in University (2008) for their financial support and assistance in this study.

References

[1] H. Arslanoglu, H.S. Altundogan, F. Tumen, Heavy metals binding properties of esterified lemon, J. Hazard. Mater. 164 (2009) 1406–1413.
[2] S. Mauchauffée, E. Meux, Use of sodium decanoate for selective precipitation of metals contained in industrial wastewater, Chemosphere 69 (2007) 763–768.
[3] L. Melita, M. Popescu, Removal of Cr (VI) from industrial water effluents and surface waters using activated composite membranes, J. Membr. Sci. 312 (2008) 157–162.
[4] C.A. Basha, N.S. Bhadrinarayana, N. Anantharaman, K.M. Meera Sheriffa Begum, Heavy metal removal from copper smelting effluent using electrochemical cylindrical flow reactor, J. Hazard. Mater. 152 (2008) 71–78.
[5] C.H. Xiong, C.P. Yao, Study on the adsorption of cadmium(II) from aqueous solution by D152 resin, J. Hazard. Mater. 166 (2009) 815–820.
[6] C.Y. Chen, C.L. Chiang, P.C. Huang, Adsorptions of heavy metal ions by a magnetic chelating resin containing hydroxy and iminodiacetate groups, Sep. Purif. Technol. 50 (2006) 15–21.
[7] N.M. Abd El-Moniem, M.R. El-Sourougy, D.A.F. Shaaban, Heavy metal ions removal by chelating resin, Pigment Resin Technol. 34 (2005) 332–339.
[8] E. Pehlivan, T. Altun, The study of various parameters affecting the ion exchange of Cu^{2+}, Zn^{2+}, Ni^{2+}, Cd^{2+} and Pb^{2+} from aqueous solution on Dowex 50W synthetic resin, J. Hazard. Mater. B134 (2006) 149–156.
[9] I. Karadjova, Determination of Cd, Co, Cr, Cu, Fe, Mn, Ni and Pb in natural waters, alkali and alkaline earth salts by electrothermal atomic adsorption spectrometry after preconcentration by column solid phase extraction, Mikrochim. Acta 130 (1999) 185–190.
[10] J.F. Dingman, K.M. Gloss, E.A. Milano, S. Siggia, Concentration of heavy metals by complexation on dithiocarbamate resins, Anal. Chem. 46 (1974) 774–777.
[11] M.E. Mahmoud, M.M. El-Essawi, E.M.I. Fathallah, Characterization of surface modification, thermal stability, and metal selectivity properties of silica gel phases-immobilized dithiocarbamate derivatives, J. Liq. Chromatogr. Related Technol. 27 (2004) 1711–1727.

[12] K.A. Venkatesan, T.G. Srinivasan, P.R. Vasudeva Rao, Removal of complexed mercury from aqueous solutions using dithiocarbamate grafted on silica gel, Sep. Sci. Technol. 37 (2002) 1417–1429.
[13] K. Dimos, P. Stathi, M.A. Karakassides, Y. Deligiannakis, Synthesis and characterization of hybrid MCM-41 materials for heavy metal adsorption, Microporous Mesoporous. Mater. 126 (2009) 65–71.
[14] S. G-Renaudin, F. Gaslain, C. Marichal, B. Lebeau, R. Schneider, A. Walcarius, Synthesis of dithiocarbamate-functionalized mesoporous silica-based materials: interest of one-step grafting, New J. Chem. 33 (2009) 528–537.
[15] B. Mathew, V.N.R. Pillai, Divinylbenzene-crosslinked polyacrylamide-supported dithiocarbamates as metal complexing agents, Polymer Bull. 26 (1991) 603–610.
[16] A. Denizli, K. Kesenci, Y. Arica, E. Pişkin, Dithiocarbamate-incorporated monosize polystyrene microspheres for selective removal of mercury ions, React. Funct. Polym. 44 (2000) 235–243.
[17] H.A. Claessens, M.A. van Straten, J.J. Kirkland, Effect of buffers on silica-based column stability in reversed-phase high-performance liquid chromatography, J. Chromatogr. A 728 (1996) 259–270.
[18] M.E. Mahmoud, Selective solid phase extraction of mercury(II) by silica gel-immobilized-dithiocarbamate derivatives, Anal. Chim. Acta 398 (1999) 297–304.
[19] S.G. Renaudin, R. Schneider, A. Walcarius, Synthesis of new dithiocarbamate-based organosilanes for grafting on silica, Tetrahedron Lett. 48 (2007) 2113–2116.
[20] S.T. Beatty, R.J. Fischer, E. Rosenberg, Comparison of novel and patented silica-polyamine composite materials as aqueous heavy metal ion recovery materials, Sep. Sci. Technol. 34 (1999) 2723–2739.
[21] H.L. Zheng, X.P. Sun, Q. He, K. Liang, P. Zhang, Synthesis and trapping properties of dithiocarbamate macromolecule heavy-metal flocculants, J. Appl. Polym. Sci. 110 (2008) 2461–2466.
[22] A.G.S. Prado, C. Airoldi, The pesticide 3-(3,4-dichlorophenyl)-1, 1-dimethylurea (Diuron) immobilized on silica gel surface, J. Colloid. Interface Sci. 236 (2001) 161–165.
[23] A. McClain, Y.-L. Hsieh, Synthesis of polystyrene-supported dithiocarbamates and their complexation with metal ions, J. Appl. Polym. Sci. 92 (2004) 218–225.
[24] X.S. Jing, F.Q. Liu, X. Yang, P.P. Ling, L.J. Li, C. Long, A.M. Li, Adsorption performances and mechanisms of the newly synthesized *N,N′*-di(carboxymethyl) dithiocarbamate chelating resin toward divalent heavy metal ions from aqueous media, J. Hazard. Mater. 167 (2009) 589–596.
[25] E. Repo, T.A. Kurniawan, J.K. Warchol, M.E.T. Sillanpää, Removal of Co(II) and Ni(II) ions from contaminated water using silica gel functionalized with EDTA and/or DTPA as chelating agents, J. Hazard. Mater. 171 (2009) 1071–1080.
[26] E.M. Tyapochkin, E.I. Kozliak, Kinetic and binding studies of the thiolate-cobalt tetrasulfophthalocyanine anaerobic reaction as a subset of the Merox process, J. Mol. Catal. A: Chem. 242 (2005) 1–17.
[27] D.J. Halls, The properties of dithioearbamates, Mikrochim. Acta (1969) 62–77.
[28] E. Humeres, N.A. Debacher, M.M. de, S. Sierra, J.D. Franco, A. Schutz, Mechanisms of acid decomposition of dithiocarbamates. 1. Alkyl dithiocarbamates, J. Org. Chem. 63 (1998) 1598–1603.
[29] E. Humeres, N.A. Debacher, M. Marta de, S. Sierra, Mechanisms of acid decomposition of dithiocarbamates. 2. Efficiency of the intramolecular general acid catalysis, J. Org. Chem. 64 (1999) 1807–1813.
[30] N. Ünlü, M. Ersoz, Removal of heavy metal ions by using dithiocarbamated-sporopollenin, Sep. Purif. Technol. 52 (2007) 461–469.
[31] P.K. Roy, A.S. Rawat, P.K. Rai, Synthesis, characterisation and evaluation of polydithiocarbamate resin supported on macroreticular styrene-divinylbenzene copolymer for the removal of trace and heavy metal ions, Talanta 59 (2003) 239–246.
[32] P. Stathi, K. Dimos, M.A. Karakassides, Y. Deligiannakis, Mechanism of heavy metal uptake by a hybrid MCM-41 material: surface complexation and EPR spectroscopic study, J. Colloid Interface Sci. 343 (2010) 374–380.
[33] R. Say, E. Birlik, Z. Erdemgil, A. Denizli, A. Ersöz, Removal of mercury species with dithiocarbamate-anchored polymer/organosmectite composites, J. Hazard. Mater. 150 (2008) 560–564.
[34] R. Say, E. Birlik, A. Denizli, A. Ersöz, Removal of heavy metal ions by dithiocarbamate-anchored polymer/organosmectite composites, Appl. Clay Sci. 31 (2006) 298–305.
[35] S. Lagergren, Zur theorie der sogenannten adsorption geloster stoffe, K. Sven. Vetenskapsakad. Handl. 24 (1898) 1–39.
[36] Y.S. Ho, G. McKay, Pseudo-second order model for sorption processes, Process. Biochem. 34 (1999) 451–465.
[37] V.C. Taty-Costodes, H. Fauduet, C. Porte, A. Delacroix, Removal of Cd(II) and Pb(II) ions, from aqueous solutions, by adsorption onto sawdust of *Pinus sylvestris*, J. Hazard. Mater. B105 (2003) 121–142.
[38] N. Ünlü, M. Ersoz, Adsorption characteristics of heavy metal ions onto a low cost biopolymeric sorbent from aqueous solutions, J. Hazard. Mater. B136 (2006) 272–280.
[39] İ.H. Gubbuk, R. Gup, H. Kara, M. Ersoz, Adsorption of Cu(II) onto silica gel-immobilized Schiff base derivative, Desalination 249 (2009) 1243–1248.
[40] I. Langmuir, The adsorption of gases on plane surfaces of glass, mica and platinum, J. Am. Chem. Soc. 40 (1918) 1361–1403.
[41] H. Freundlich, Ueber die adsorption in loesungen, Z. Physik. Chem. 57 (1907) 385–470.
[42] H. Dikici, K. Saltali, Equilibrium and kinetics characteristics of copper (II) sorption onto gyttja, Bull. Environ. Contam. Toxicol. 84 (2010) 147–151.
[43] M.M. Dubinin, L.V. Radushkevich, Equation of the characteristic curve of activated charcoal, Proc. Acad. Sci. Phys. Chem. Sect. U.S.S.R. 55 (1947) 331–333.
[44] N.D. Hutson, R.T. Yang, Theoretical basis for the Dubinin–Radushkevitch (D–R) adsorption isotherm equation, Adsorption 3 (1997) 189–195.
[45] J.P. Hobson, Physical adsorption isotherms extending from ultrahigh vacuum to vapor pressure, J. Phys. Chem. 73 (1969) 2720–2727.
[46] M.S. Onyango, Y. Kojima, O. Aoyi, E.C. Bernardo, H. Matsuda, Adsorption equilibrium modeling and solution chemistry dependence of fluoride removal from water by trivalent-cation-exchanged zeolite F-9, J. Colloid Interface Sci. 279 (2004) 341–350.
[47] R. Payne, R.J. Magee, J. Liesegang, Infrared and X-ray photoelectron spectroscopy of some transition metal dithiocarbamates and xanthates, J. Electron. Spectrosc. Relat. Phenom. 35 (1985) 113–130.
[48] J.A. Gardella, S.A. Ferguson, R.L. Chin, $\pi^* \leftarrow \pi$ Shakeup satellites for the analysis of structure and bonding in aromatic polymers by X-Ray Photoelectron Spectroscopy, Appl. Spectrosc. 40 (1986) 224–232.
[49] P. Morf, F. Raimondi, H.G. Nothofer, B. Schnyder, A. Yasuda, J.M. Wessels, T.A. Jung, Dithiocarbamates: functional and versatile linkers for the formation of self-assembled monolayers, Langmuir 22 (2006) 658–663.
[50] C. Ji, S. Song, C. Wang, C.M. Sun, R.J. Qu, C.H. Wang, H. Chen, Preparation and adsorption properties of chelating resins containing 3-aminopyridine and hydrophilic spacer arm for Hg(II), Chem. Eng. J. 165 (2010) 573–580.
[51] M. Saad, C. Gaiani, M. Mullet, J. Scher, B. Cuq, X-ray Photoelectron Spectroscopy for wheat powders: measurement of surface chemical composition, J. Agric. Food Chem. 59 (2011) 1527–1540.
[52] E.O. Guareno, F.S. Gutiérrez, J.L.M. Quiroz, S.L.H. Olmos, V. Soto, W. Cruz, R. Manríquez, S.G. Salazar, Removal of Cu(II) ions from aqueous streams using poly(acrylic acid-co-acrylamide) hydrogels, J. Colloid Interface Sci. 349 (2010) 583–593.
[53] J. Dong, Z.H. Xu, F. Wang, Engineering and characterization of mesoporous silica-coated magnetic particles for mercury removal from industrial effluents, Appl. Surf. Sci. 254 (2008) 3522–3530.
[54] B. Kannamba, K. Laxma Reddy, B.V. AppaRao, Removal of Cu(II) from aqueous solutions using chemically modified chitosan, J. Hazard. Mater. 175 (2010) 939–948.
[55] C. Liu, R. Bai, Q.S. Ly, Selective removal of copper and lead ions by diethylenetriamine-functionalized adsorbent: behaviors and mechanisms, Water Res. 42 (2008) 1511–1522.
[56] S. Biniak, M. Pakula, G.S. Szymanski, A. Swiatkowski, Effect of activated carbon surface oxygen and/or nitrogen containing groups on adsorption of copper(II) ions from aqueous solution, Langmuir 15 (1999) 6117–6122.
[57] T.J. Zhu, X-ray diffraction and photoelectron spectroscopic studies of (0 0 1)-oriented $Pb(Zr_{0.52}Ti_{0.48})O_3$ thin films prepared by laser ablation, J. Appl. Phys. 95 (2004) 241–247.
[58] D.W. Niles, G. Herdt, M. Al-Jassim, An X-ray photoelectron spectroscopy investigation of O impurity chemistry in CdS thin films grown by chemical bath deposition, J. Appl. Phys. 81 (1997) 1978–1985.
[59] S. Thirumaran, K. Ramalingam, G. Bocelli, L. Righi, XPS, single crystal X-ray diffraction and cyclic voltammetric studies on 1,10-phenanthroline and 2,2′-bipyridine adducts of bis(piperidinecarbodithioato-S,S′) cadmium(II) with CdS_4N_2 environment—a stereochemical and electronic distribution investigation, Polyhedron 28 (2009) 263–268.
[60] R. Payne, R.J. Magee, Chemical shits in transition metal dithiocarbamates from infrared and X-ray photoelectron spectroscopies, Chem. Phys. Lett. 93 (1982) 103–106.
[61] J.M. Smith, Chemical Engineering Kinetics, third ed., McGraw-Hill, New York, 1981, pp. 310–322.